Proceedings of the National Conference on Computational Modeling of Fluid Dynamics Problems (CMFDP-2019)
NIT Warangal, India – Jan 18-20, 2019
Paper No. XXX (The number assigned when the papaer is accepted)

Computational Modeling of Gas-to-Solid Heat Transfer in an Adiabatic, Vertical Pipe

Brundaban Patro1[a,*], K. Kiran Kumar2[a], D. Jaya Krishna3[a]
[a]*Department of Mechanical Engineering, National Institute of Technology Warangal, Warangal-506004, Telangana, India*

*Corresponding author Email: bpatro111@gmail.com

Received: Date? Accepted: Date?

Gas-solid flows in vertical pipes are found in many industries for heat transfer applications. Some of them are chemical industries, food and process industries, pharmaceutical industries, etc. In the present paper, the two-fluid model (the Eulerian-Eulerian approach) of Ansys Fluent 15.0 is used to model the heat transfer in gas-solid flows in an adiabatic, vertical pipe. The variable gas properties with respect to temperature are considered in the present study. The computational results are well validated with the benchmark experimental data. The effect of particle diameter on heat transfer and pressure drop is studied. It is noticed that the gas temperature increases and the solid temperature decreases with increasing the particle diameter. Again, increasing the particle diameter increases the logarithmic mean temperature difference and pressure drop; however, it decreases the average gas-solid Nusselt number.

***Keywords*:** Gas-solid flows; heat transfer, numerical modeling, logarithmic mean temperature difference.

1. Introduction

Gas-solid flows in vertical pipes are found in many industries for heat transfer applications. Some of them are chemical industries, food and process industries, pharmaceutical industries, etc. Many authors[1-8] experimentally studied thermo-hydrodynamic characteristics of gas-solid flows using heated walls in vertical pipes. Rajan et al.[9] studied air to solid heat transfer during pneumatic conveying in an adiabatic, vertical pipe using gypsum as the solid material. They studied the effects of solid feed rate, air velocity, and particle size on heat transfer. Mokhtarifar et al.[10] experimentally studied gas-solid heat transfer in adiabatic pipes and found that increasing the solid loading ratio (SLR) results in decreasing the gas-solid Nusselt number and solid temperature in a dilute regime, and it results in their growth in a dense regime.

Due to rapid advancement in computer science and information technology, numerical studies, as an alternative method, are also useful to obtaining the fluid dynamics results. There are two numerical approaches, i.e., the Eulerian-Lagrangian approach and the Eulerian-Eulerian approach in gas-solid flow modeling. The Eulerian-Lagrangian approach treats the gas phase as continuous and the solid phase as discrete phase. However, the Eulerian-Eulerian approach treats both the phases as inter-penetrating continua. Many authors[11-18] used the Eulerian-Lagrangian approach and many other authors[19-22] used the Eulerian-Eulerian approach to study the wall to suspension heat transfer in vertical pipes. Rajan et al.[23] studied heat transfer between cold particles and hot air using plastic pellets of size 0.2 mm to 2 mm using the Eulerian-Eulerian approach in pneumatic conveying. They noticed the influence of particle size on flow behavior and heat transfer. Bourloutski et al.[24] compared the above two approaches of numerical modeling in gas-solid flows in a pipe and concluded that the Lagrangian approach is limited to small SLRs (2-3), and the time required to reach the converged solution is 3-5 times more than the Eulerian-Eulerian approach. Using both numerically (the Eulerian-Lagrangian approach) and experimentally, El-Behery et al.[25] studied

heat transfer during vertical pneumatic transport. They used hot gas with cold limestone particles and cold gas with hot limestone particles in their study. They found that the temperature of the two-phases increases as the Reynolds number increases and the SLR deceases. They also noticed that the pressure drop increases in dilute phase and decreases in dense phase when the hot particles are introduced in the cold gas flow, and an opposite effect is noticed when the cold particles are introduced in the hot gas flow. Moreover, El-Behery et al.[26] modeled the gas-solid flows with heat transfer using the steady state one-dimensional Eulerian-Eulerian approach, and it was found that the model is capable of modeling compressible gas-solid flows with heat transfer. They noticed that the pressure drop increases as the SLR, solid diameter, and solid density increase.

There are limited published research works on heat transfer in gas-solid flows subjected to adiabatic walls, where the heat transfer takes place from hot gas to cold solids. Again, the thermal interactions between gas and solid phases are yet not well understood in these systems. Therefore, in the present study, an attempt is taken to study the heat transfer (from hot gas to cold solids) in a vertical pipe having an adiabatic wall. In the present study, the Eulerian-Eulerian approach is employed with temperature variable gas properties.

2. Mathematical Model and Numerical Procedure

Assuming no mass transfer between the phases or source terms, the continuity equation for gas phase and solid phase is

$$\frac{\partial}{\partial t}(\alpha_i \rho_i) + \nabla \cdot (\alpha_i \rho_i v_i) = 0 \quad (1)$$

where 'i' is either gas or solid and $\sum \alpha_i = 1$.

Neglecting virtual mass force and external body forces, the momentum equation for gas phase is

$$\frac{\partial}{\partial t}(\alpha_g \rho_g v_g) + \nabla \cdot (\alpha_g \rho_g v_g v_g) = -\alpha_g \nabla \bar{p} + \nabla \cdot \tau_g + \alpha_g \rho_g g + K_{sg}(v_s - v_g) \quad (2)$$

and the momentum equation for solid phase is

$$\frac{\partial}{\partial t}(\alpha_s \rho_s v_s) + \nabla \cdot (\alpha_s \rho_s v_s v_s) = -\alpha_s \nabla \bar{p} - \nabla \bar{p_s} + \nabla \cdot \tau_s + \alpha_s \rho_s g + K_{gs}(v_g - v_s) \quad (3)$$

Neglecting the radiation heat transfer, the energy equation for gas phase is

$$\alpha_g \rho_g C_{pg}\left(\frac{\partial T_g}{\partial t} + v_g . \nabla T_g\right) = -\nabla . q_g + h(T_s - T_g) \quad (4)$$

and the energy equation for solid phase is

$$\alpha_s \rho_s C_{ps}\left(\frac{\partial T_s}{\partial t} + v_s . \nabla T_s\right) = -\nabla . q_s - h(T_s - T_g) \quad (5)$$

The various constitutive equations, which are required in the mathematical modelling, are presented in Table 1. Stress tensors (τ) are

$$\tau_g = \alpha_g \mu_g (\nabla v_g + \nabla v_g^T) + \alpha_g \left(\lambda_g - \frac{2}{3}\mu_g\right) \nabla . v_g I \quad (6)$$

$$\tau_s = \alpha_s \mu_s (\nabla v_s + \nabla v_s^T) + \alpha_s \left(\lambda_s - \frac{2}{3}\mu_s\right) \nabla . v_s I \quad (7)$$

The granular shear viscosity is a combination of viscosities due to kinetic motion and collision interaction between particles.

$$\mu_s = \mu_{s,kin} + \mu_{s,coll} \quad (8)$$

The gas-solid heat transfer coefficient (h) is, $h = \frac{6 k_g \alpha_s \alpha_g Nu_s}{d_s^2}$ (9)

Properties of gas, i.e., density, dynamic viscosity, thermal conductivity and specific heat are defined with respect to temperature.

$$\rho_g = \frac{\mathrm{P}}{\mathrm{R_A T_K}} \tag{10}$$

where P is the absolute pressure (Pa) at atmospheric conditions. A temperature dependent piecewise-polynomial profile is used to define the normal dynamic viscosity of gas (μ_{gn})[27].

$$\mu_{gn} = \mathrm{A} - \mathrm{BT} + \mathrm{CT^2} - \mathrm{DT^3} + \mathrm{ET^4} - \mathrm{FT^5} + \mathrm{GT^6} - \mathrm{HT^7} \tag{11}$$

where A, B, C, D, E, F, G and H are the coefficients, and A=1161.482, B=2.368819, C=0.01485511, D=5.034909×10^{-05}, E=9.928569×10^{-08}, F=1.111097×10^{-10}, G=6.540196×10^{-14}, H=1.573588×10^{-17}.

Two separate user defined functions are provided to define the gas phase thermal conductivity (k_g) and specific heat at constant pressure ($C_P g$) as per Eq. 12 and Eq. 13, respectively[28].

$$\mathrm{k_g} = 0.02624\left(\frac{\mathrm{T_K}}{300}\right)^{0.8646} \tag{12}$$

$$\mathrm{C_{Pg}} = 1002.5 + 275 \text{ x } 10^{-6}(T_K - 200)^2 \tag{13}$$

Table 1. Different models used in constitutive equations

Terms	Models used
Granular bulk viscosity (λ_s)	Lun et al.[29]
Granular viscosity (μ_s)	Syamlal et al.[30]
Solid pressure	Lun et al.[29]
Radial distribution function	Lun et al.[29]
Turbulence	Standard $k-\varepsilon$ turbulence model[31]
Granular temperature	PDE granular temperature model[32]
Drag force	When $\alpha_g > 0.8$, Wen and Yu model[33]
	But when $\alpha_g \leq 0.8$, Ergun model[34]
Particle Nusselt number	Gunn model[35]

A fully developed velocity profile boundary condition is used for gas phase at the inlet. However, a uniform axial velocity profile (equal to gas velocity) is used for solid phase at the inlet. The outflow boundary condition is used for both the phases at the outlet. A no-slip wall boundary condition is used for gas phase, and a partial-slip wall boundary condition as given by Johnson and Jackson[36] with a specularity coefficient 0.05 is used for solid phase. Particle-particle and particle-wall restitution coefficients are taken as 0.9 and 0.95, respectively. The wall is specified at the adiabatic condition.

The commercial software package Ansys 15.0 is used for geometric modeling (a vertical pipe of internal diameter 58 mm and length 6 m), meshing, and transient simulations. For the pressure and velocity coupling, the PC-SIMPLE (phase coupled semi-implicit method for pressure linked equations) algorithm is used. For the momentum and energy equations, a second-order upwind scheme, and for the volume fraction equations, the QUICK (quadratic upstream interpolation for convective kinetics) scheme are used. For the turbulent kinetic energy, turbulent energy dissipation rate, and granular temperature equations, a first-order upwind scheme is used. A convergence criteria of 10^{-3} are used for all.

3. Data Reduction

The average gas-solid Nusselt number is calculated as explained below. From the energy balance

$$\dot{m}_g C_{pg}\left(T_{g,in} - T_{g,out}\right) + \dot{m}_s C_{ps}\left(T_{s,in} - T_{s,out}\right) = 0 \quad (14)$$

The overall gas-solid heat transfer coefficient (U) is calculated as

$$\dot{m}_g C_{pg}\left(T_{g,in} - T_{g,out}\right) = UA_s(LMTD) \quad (15)$$

The heat transfer area can be calculated as

$$A_s = 6M_s/(\rho_s . d_s) \quad (16)$$

Here, M_s is the solid holdup and can be calculated as

$$M_s = (\dot{m}_s . \Delta z)/v \quad (17)$$

The logarithmic mean temperature difference (LMTD) is calculated as

$$LMTD = (\Delta T_{in} - \Delta T_{out})/(\ln(\Delta T_{in}/\Delta T_{out})) \quad (18)$$

$$\Delta T_{in} = T_{g,in} - T_{s,in} \quad (19)$$

$$\Delta T_{out} = T_{g,out} - T_{s,out} \quad (20)$$

The local gas-solid Nusselt number (Nu_l) is calculated as

$$Nu_l = UD/k_g \quad (21)$$

The average gas-solid Nusselt (Nu_{avg}) number is calculated as

$$Nu_{avg} = \int_0^L Nu_l . dz/L \quad (22)$$

4. Results and Discussion

The present numerical results for average SLR and average gas-solid Nusselt number are compared with the experimental results of Mokhtarifar et al.[10] and are plotted in Fig. 1a and Fig. 1b, respectively. In this, air is used as the gas phase and sand (density 1500 kg/m^3, specific heat 800 J/kgK, thermal conductivity 0.8 W/mK) is used as the solid phase. The mean gas velocity is 18.5 m/s, and sand particles are of 253 micron in size. The inlet air temperature is 443.15 K, and the inlet solid temperature is 308.15 K. It is noticed from both the figures that the present numerical results agree well with the experimental results of Mokhtarifar et al.[10]. The present numerical results show a maximum deviation of 3% for the average SLR and a maximum deviation of 6% for the average gas-solid Nusselt number with the benchmark experimental data.

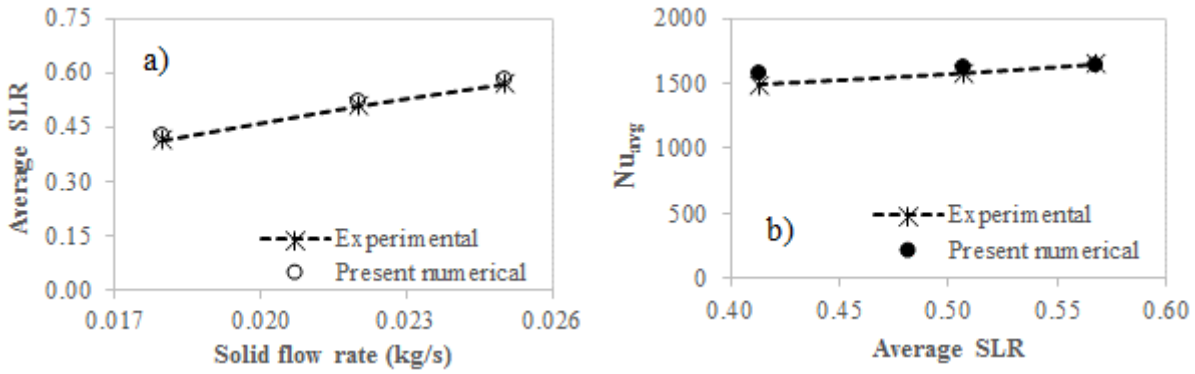

Fig. 1. Comparison of present numerical results with the experimental results of Mokhtarifar et al.[10] for average SLR and average gas-solid Nusselt number

Now the parametric studies are conducted using the simulation considering different particle sizes such as 100 micron, 200 micron, and 300 micron. The mean gas velocity is 18 m/s (inlet gas Reynolds number 33850), and the SLR at the inlet is 0.7. The effects of particle diameter on gas and solid temperatures, LMTD, average gas-solid Nusselt number, and pressure drop are studied.

The effect of particle diameter on gas and solid temperatures at a distance 0.5 m from the inlet is shown in Fig. 2. It is observed from Fig. 2 that the gas temperature increases and the solid temperature decreases with increasing the particle diameter. This is due to decrease in the particle residence time. Particle residence time decreases with increasing the particle diameter due to less number of particles.

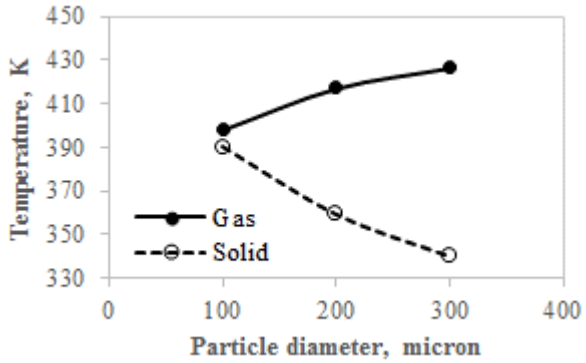

Fig. 2. Effect of particle diameter on gas and solid temperatures

The effect of particle diameter on LMTD is shown in Fig. 3a. It is observed from Fig. 3a that the LMTD increases with increasing the particle diameter. By increasing the particle diameter, the gas temperature increases and the solid temperature decreases. Therefore, the temperature difference between gas and solid increases, which increases the LMTD.

The effect of particle diameter on average gas-solid Nusselt number is shown in Fig. 3b. It is observed from Fig. 3b that the gas-solid Nusselt number decreases with increasing the particle diameter. This is due to turbulence suppression by the solid particles with increasing the particle diameter.

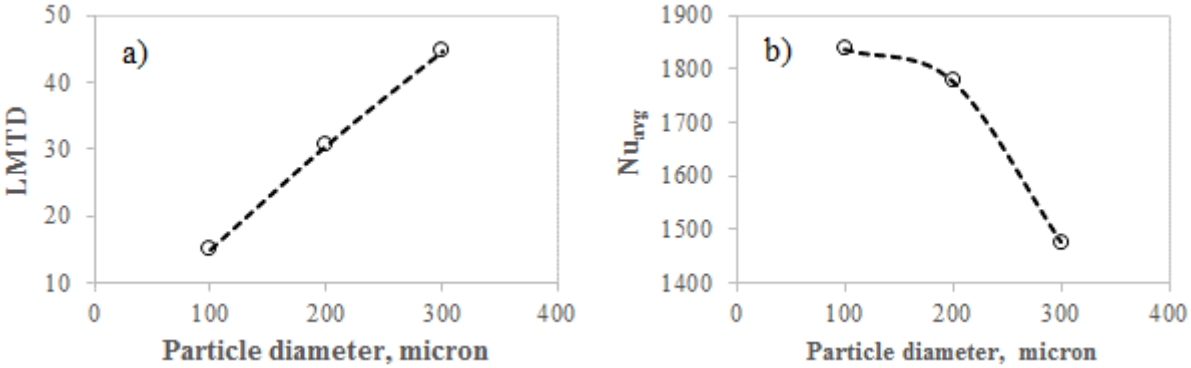

Fig. 3. Effect of particle diameter on LMTD and average gas-solid Nusselt number

The effect of particle diameter on pressure drop is shown in Fig. 4. It is observed from Fig. 4 that the pressure drop increases with increasing the particle diameter. Increasing the particle diameter increases the slip velocity between gas and solid phases, and the increased slip velocity increases the drag force. Therefore, the pressure drop increases with increasing the particle diameter.

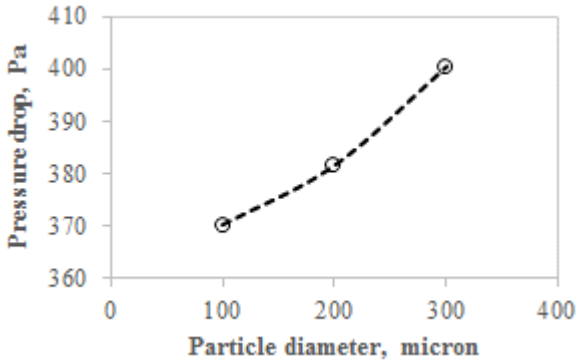

Fig. 4. Effect of particle diameter on pressure drop

5. Conclusion

In the present paper, computational modeling of gas-solid flows through a three-dimensional vertical pipe having an adiabatic wall is carried out, using the two-fluid model (Eulerian-Eulerian approach) of Ansys Fluent 15.0. It is known that the gas properties vary with temperature and affect the fluid dynamics study. Therefore, the properties of gas are defined as per the temperature variation along the length of the pipe. First, the computational results are validated with the benchmark experimental data. The computational results show a maximum deviation of 6% with the benchmark experimental data for the average gas-solid Nusselt number. Then, the parametric studies are carried out using the particle diameter ranging from 100 micron to 300 micron at the mean gas velocity 18 m/s and inlet SLR 0.7. It is noticed that the gas temperature increases and the solid temperature decreases with increasing the particle diameter. Increasing the particle diameter increases the LMTD and pressure drop; however, it decreases the average gas-solid Nusselt number.

Nomenclature

A_s	heat transfer area of particles (m^2)
C_p	constant pressure specific heat (J/kgK)
d_s	particle diameter (m)
D	diameter of the pipe (m)
g	acceleration due to gravity (m/s^2)
h	gas-solid heat transfer coefficient (W/m^2K)
I	unit tensor
k_g	thermal conductivity (W/mK)
K_{gs}, K_{sg}	gas-solid momentum exchange coefficient (kg/m^3s)
L	length of the pipe (m)
$\dot{m}$	mass flow rate (kg/s)
M_s	solid holdup (kg)
Nu	gas-solid Nusselt number
Nu_s	particle Nusselt number
P	absolute pressure (Pa)
$\bar{p}$	mean pressure (Pa)
R_A	specific gas constant (J/kgK)
T, T_K	temperature (K)
ΔT	temperature difference between gas and solid (K)
q	heat flux (W/m^2)
v	mean velocity (m/s)

U	overall heat transfer coefficient (W/m^2K)
z	axial distance (m)
Δz	distance from particle feeding point (m)
LMTD	logarithmic mean temperature difference
SLR	solid loading ratio
α	volume fraction
λ	bulk viscosity (kg/ms)
μ	shear viscosity (kg/ms)
μ_{gn}	normal dynamic viscosity of gas (kg/ms)
ρ	density (kg/m^3)
τ	stress-strain tensor (kg/ms^2)

Subscripts

i	gas or solid
avg	average
g	gas
in	inlet
l	local
out	outlet
s	solid

References

[1] L. Farbar and M. J. Morley, Ind. Eng. Chem. 49, 1143 (1957).
[2] C. A. Depew and L. Farbar, J. Heat Transfer, 164 (1963).
[3] L. Farbar and C. A. Depew, Ind. Eng. Chem. Fundam. 2, 130 (1963).
[4] R. G. Boothroyd and H. Haquet, J. Mech. Eng. Sci. 12, 191 (1970).
[5] M. K. Wahi, J. Heat Transfer, 145 (1977).
[6] S. Matsumoto, S. Ohnishi, and S. Maeda, J. Chem. Eng. Jpn. 11, 89 (1978).
[7] R. S. Kane and R. Pfeffer, J. Heat Transfer 107, 570 (1985).
[8] R. A. Sorensen, J. D. Seader, and B. S. Brewster, Ind. Eng. Chem. Res. 40, 457 (2001).
[9] K. S. Rajan, K. Dhasandhan, S. N. Srivastava, and B. Pitchumani, Int. J. Heat Mass Transfer 51, 2801 (2008).
[10] N. Mokhtarifar, F. Saffaraval, M. Saffar-Avval, Z. Mansoori, and A. Siamie, Heat Transfer Eng. 36, 113 (2015).
[11] R. Avila and J. Cervantes, Int. J. Heat Mass Transfer 38, 1923 (1995).
[12] Z. Mansoori, M. Saffar-Avval, H. B. Tabrizi, G. Ahmadi, and S. Lain, Int. J. Heat Fluid Flow 23, 792 (2002).
[13] V. Chagras, B. Oesterle, and P. Boulet, Int. J. Heat Mass Transfer 48, 1649 (2005).
[14] M. Saffar-Avval, H. B. Tabrizi, Z. Mansoori, and P. Ramezani, Int. J. Therm. Sci. 46, 67 (2007).
[15] M. Haim, Y. Weiss, and H. Kalman, Part. Sci. Technol. 25, 173 (2007).
[16] F. Behzad, Z. Mansoori, M. Saffar-Avval, H. B. Tabrizi, and G. Ahmadi, Int. J. Heat Mass Transfer 53, 1175 (2010).
[17] S. M. El-Behery, W.A. El-Askary, M. H. Hamed, and K. A. Ibrahim, Int. J. Heat Fluid Flow 32, 740 (2011).
[18] M. Pishvar, M. Saffar Avval, Z. Mansoori, and M. Amirkhosravi, Powder Technol. 262, 223 (2014).
[19] K. S. Han, H. J. Sung, and M. K. Chung, Int. J. Heat Mass Transfer 34, 69 (1991).
[20] P. Boulet, B. Oesterle, and A. Taniere, Part. Sci. Technol. 17, 253 (1999).

[21] S. Azizi, M. Taheri, and D. Mowla, Numer. Heat Transfer, Part A 62, 659 (2012).
[22] P. Patro, Drying Technol. 34, 703 (2015).
[23] K. S. Rajan, B. Pitchumani, S. N. Srivastava, and B. Mohanty, Int. J. Heat Mass Transfer 50, 967 (2007).
[24] E. S. Bourloutski, A. M. Bubenchikov, and A. V. Starchenko, Mech. Res. Commun. 29, 437 (2002).
[25] S. M. El-Behery. W. A. El-Askary, M. H. Hamed, and K. A. Ibrahim, Int. J. Heat Fluid Flow 33, 118 (2012).
[26] S. M. El-Behery. A. A. El-Haroun, and M. R. Abuhegazy, J. Appl. Fluid Mech. 10, 519 (2017).
[27] Fluent Inc., Fluent User Guide, Lebanon, NH, USA, (2003) (currently ANSYS Inc., Canonsburg, PA, USA).
[28] J. C. Dixon, The Shock Absorber Handbook, Second Ed., John Wiley & Sons Ltd., England (2007).
[29] C. K. K. Lun, S. B. Savage, D. J. Jeffrey, and N. Chepurniy, J. Fluid Mech. 140, 223 (1984).
[30] M. Syamlal, W. Rogers, and T. J. O`Brien, MFIX documentation: Theory guide. DOE/METC-94/1004, Department of Energy, Morgantown Energy Technology Center, Morgantown, WV, (1993).
[31] B. E. Launder and D. B. Spalding, Comput. Methods Appl. Mech. Eng. 3, 269 (1974).
[32] J. Ding and D. Gidaspow, AIChE J. 36, 523 (1990).
[33] C. Y. Wen and Y. H. Yu, Chem. Eng. Prog. Symp. Ser. 162, 100 (1966).
[34] S. Ergun, Chem. Eng. Prog. 48, 89 (1952).
[35] D. J. Gunn, Int. J. Heat Mass Transfer 21, 467 (1978).
[36] P. C. Johnson and R. Jackson, J. Fluid Mech. 176, 67 (1987).